An Approach to Realisation of a Radial Phase Mask using 3-D Printing in Transparent PLA

Simran Agarwal[*1], Non-member,
Romuald Jolivot[*], Non-member, and **Waleed S. Mohammed**[*], Non-member

ABSTRACT

In the recent years, many different techniques and algorithms have been devised to design diffractive optical elements (DOE's) for the purpose of beam shaping. This paper demonstrates an approach to realise a 3-D printed radial phase mask to be used in beam shaping to achieve a beam profile closer to the flattop. An iterative algorithm approach is employed to simulate the phase masks in greyscale and subsequently into STL format. These 3-D printed masks are used as an optical element and characterised using an experimental setup. The images of the light after the characterisation are examined and compared with the simulated results. Therefore, this method reduces the complexity as 3-D printing the masks eliminates the need for fabrication, processing time and number of components necessary to obtain a flattop beam profile.

Keywords: Beam Shaping, Gaussian Beam, Diffractive Optical Element Design, Optimisation, Flattop Beam, 3D Printing, Radial Phase Mask.

1. INTRODUCTION

Transformation of a Gaussian beam profile to different distributions of intensity profiles is an important area of research and have become more eminent since the invention of laser. Generally, the fiber or fiber-coupled sources produce a Gaussian or close to Gaussian profile. This type of light sources is typically used for applications like cutting, welding, laser patterning, laser corneal surgery and laser skin treatments. The high intensity peak at the center of a Gaussian profile can adversely affect the optical components and the workpieces. Hence, the concept of beam shaping is required where an incident beam of light is redistributed through a set of optical elements or components. It is observed in many studies that use of top-hat beam profiles having uniform energy distribution improves process quality [1, 2]. Bischoff *et al.* (2015) compares the use of Gaussian beam profile and the top-hat profile. In the case of Gaussian beam profile, the energy below the threshold value fails to contribute in the laser process and hence, results in heating problems in the material. Whereas, for the homogeneous intensity of the top-hat beam profile this loss of energy in the form of heat is minimized therefore making the process more efficient and low loss [3]. Beam shaping optics are necessary for innovative laser processing techniques and diffractive beam splitters along with top-hat beam shapers accelerate laser machining process.

Diffractive optics and holographical optical elements can be efficiently used to produce arbitrary light distributions. The transformation of Gaussian beams using diffractive optical elements (DOE's) has been known for decades. The use of both continuous and discrete phase plane elements containing two or more zones with binary phase value (usually 0 and π) were proposed for beam shaping [4, 5]. Nevertheless, the system involving DOE's can only be applicable for specific output beam profiles similar to other methods like transmissive and refractive optics. Hence, this shortcoming restricts its applications.

Hoffnagle and Jefferson [6] used a refractive optical system comprising of two aspheric lenses to align the input beam to a desired pattern. Moreover, the design supports efficient power conversion. Gerchberg and Saxton [7] designed an iterative algorithm (GS algorithm) for the phase retrieval of a field at two different planes. GS algorithm was used to evaluate the modulation function of a phase mask that produces a known far-field intensity distribution when illuminated. The distribution is subsequently used to calculate the diffractive optical elements (DOE's) that can be utilized in imaging application [8, 9]. Although, it simplifies the discretization of the phase of a DOE (for fabrication purposes), it requires the field amplitudes to be known restricting its performance. Orozco and Barbosa (2013) employed both ray tracing and Huygen-Fresnel principle to characterise a complex optical setup in order to obtain the direct and inverse propagation functions to calculate the phase mask needed to produce the intended irradiance on the output image plane [10] Gaussian beam profiles can be transformed into a flattop beam by implementing a two element refractive optical system such as the one devised by Smilie and Suleski [11]. This system possesses limitations as it is only applicable for specific input-output combinations and it is inefficient to cancel or lower the spatial noise in laser

Manuscript received on December 23, 2017 ; revised on February 4, 2018.
*The author is with Bangkok University, Center of Research in Optoelectronics, Communications and Control Systems (BU-CROCCS), E-mail : [1]simran.agarwal240@gmail.com.

beams.

Another aspect of beam-shaping is designing and fabricating the optical element once the algorithm and optimization is achieved. Conventionally, fabrication of phase masks can be realized by lithography techniques such as gray-scale, multiple-mask or moving-mask lithography accompanied by different etching processes [12]. Gissibl *et al.* (2016) demonstrates that 3D printed phase plates directly attached to optical single-mode fibers can result in spatial intensity beam shaping. Due to the profile of these phase plates there is a spatial phase shift generated and hence, can be used as focusing or beamshaping elements [13]. It has been proved that 3D printing of diffractive micro-optics can achieve sufficient performance to enable compact devices. These phase plates are fabricated by femtosecond two-photon direct laser writing using dip-in method [14]. This type of non-linear approach to fabrication, such as femtosecond laser ablation, is being widely used in fabrication of large area samples. They are time and cost intensive [15,16]. 3-D printing of micro-optics can be safely claimed to be the future of fiber optics and laser beam-shaping, laser material processing.

In our proposed design, a single radially symmetric phase mask or element is to be designed through an iterative algorithm discussed in section 2. Furthermore, it is to be optimised in order to produce a desired output intensity from the Gaussian input. The next step is to 3-D print the simulated masks using a transparent PLA. An optical setup is designed to characterise the 3-D mask and analyse the results. This beam shaping scheme reduces complexity and is low-cost.

2. REALISATION OF THE EDGE DESIGN OF THE MASK

2.1 Design of The Radial Phase Mask

The main objective of this approach is to use a single radially symmetric optical element to obtain a desired beam profile. There are two parameters that are crucial to the phenomenon of beam shaping: intensity profile and phase of the beam. The intensity profile is considered to be proportional to the absolute square of the Fourier transform of the input field at the focal point. It is assumed that the input field is the product of the Gaussian input and phase from the element. An iterative algorithm called Method of Projection (MOP) is employed for the optimisation process which aids to simulate suitable phase masks.

The block diagram of the proposed algorithm is shown in figure 1. The input to the system is a Gaussian beam (E_1) defined as:

$$E_1(r) = \exp^{\left(\frac{-r^2}{\sigma^2}\right)} \tag{1}$$

where, σ is the beam waist and r is the radial space. The initial phase ϕ of the desired element is imperially set to be a linear function of r and is given by equation (2).

$$\phi(r) = \pi \frac{-r}{\max(r)} \tag{2}$$

The selection of this initial phase instead of a random phase (shown in equation (2)) was found to fasten the convergence process. Therefore, the input field at the first step of optimization is represented as:

$$E_2(r) = E_1(r) * e^{i\phi(r)} \tag{3}$$

For the optimization of phase, method of projection is proposed. In MOP, an initial beam or field is mapped into a hypothetical two-dimensional solution space, which consists of a set of solutions. To achieve a solution inside the solution set or at its closest proximity, an iterative route involving Henkel transform is used for the forward and backward beam propagations. During this process the phase of the output field is retained and amplitude is set to unity to reach a new field.

The process is then repeated till either a solution (inside the solution space) is reached or the error is minimized. The phase from the final step is then extracted and implemented back again as the input. The closeness of the output after each iteration is evaluated through cross-correlation (section 2.2). The iteration process is repeated until a predefined value of cross-correlation or the criterion of goodness is achieved.

The element E_3(q) in figure 1 is the Radial Fourier Transform (RFT) of equation (3), where 'q' is the spatial frequency. The next step involves replacing the amplitude intensity by the desired value, which can be done by replacing it with a super-Gaussian defined by equation (4):

$$E_s(h) = e^{-[(\frac{h}{\max(h)})^5]} \tag{4}$$

where 'h' is in space which has a defined step size.

The order of the super Gaussian E_s is greater than the normal Gaussian G_1 given by equation (1), that is, order (E_s) > order (E_1), which gives a flatter and smoother beam. Further, to get the desired amplitude intensity A_d (q), it is necessary to normalize the amplitude of the Fourier transform and multiply it with the super-Gaussian as expressed by:

$$A_d(q) = \left(\frac{F_1(q)}{|(F_1(q))|}\right) \cdot E(h) \tag{5}$$

The Henkel Transform of equation (5) represents the operation of backward propagation of the beam. The output is given by G_{back} (result of the inverse Henkel transform) from which the phase is extracted

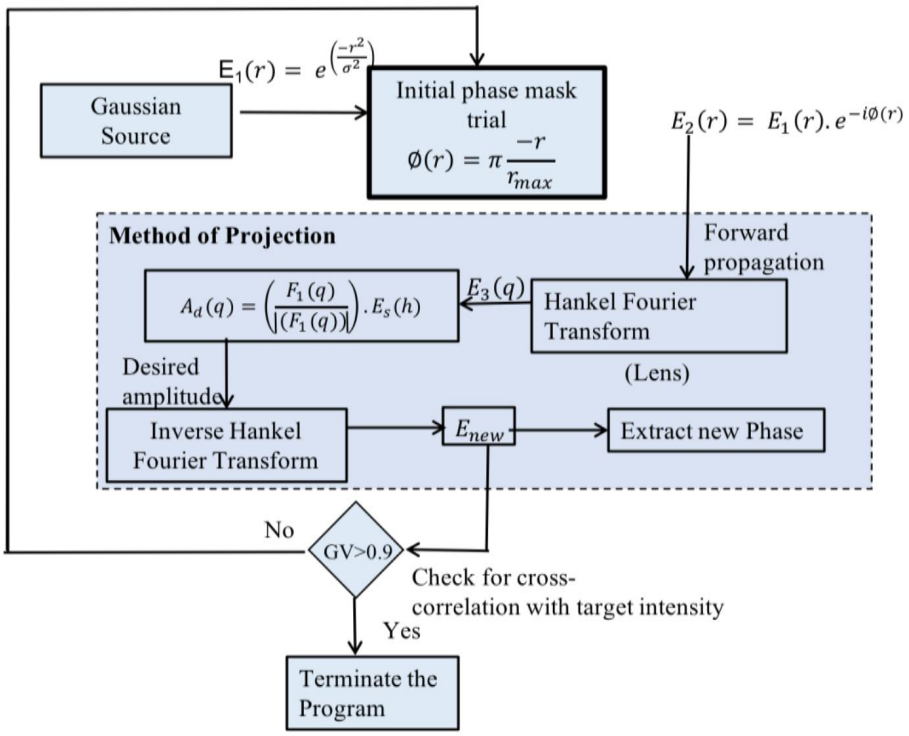

Fig.1: *Iterative algorithm to design phase mask.*

and checked for closeness with the target through cross-correlation. In case the value is lower than the goodness value (0.9), the phase goes through the iterative loop again.

In this beam-shaping approach, both the input and mask have a circular symmetry. Hence, Henkel transform is opted for instead of the cartesian two-dimensional Fourier transform for the forward and backward propagation. The input function in two dimensions defined as E_1 (x,y) is combined with phase element $e^{-i\phi(x,y)}$ to give the output form after passing the lens. It is expressed by:

$$E_F\left(u \cdot v\right) = \int \int_{-\infty}^{\infty} E_1\left(x, y\right) e^{-i2\pi(ux+vy)} dxdy \quad (6)$$

Equation (6) is then converted to cylindrical coordinates and can be expressed as a Henkel transform as:

$$E_F\left(q\right) = 2\pi \int_0^{\infty} E_1\left(r\right) J_0\left(2\pi qr\right) rdr \quad (7)$$

where, r is the radial space, $J_0(2\pi qr)$ is the zeroth -order Bessel function.

2.2 Optimisation Of Radial Phase Mask

In order to further optimise the design, it has to be ensured that the output profile is as close as possible to the target profile. This is done by the method of cross-correlation which can be expressed by equation (8) as:

$$cross_{norm} = \frac{\sum_{X=0}^{N-1} X\left[n\right] y\left[n\right]}{\sqrt{\sum_{X=0}^{N-1} X^2\left[n\right] \sum_{X=0}^{N-1} y^2\left[n\right]}} \quad (8)$$

where, $X[n]$ is a discrete function (output for our case) and $y[n]$ is another discrete function (desired output). The denominator in the above equation is the scaling factor which normalises the profile.

2.3 Relation between phase of the mask and thickness

For further optimisation and realisation of the 3-D printed mask from the greyscale relation of the thickness of the profile to be printed and the phase of the mask is of importance. The phase can be mathematically derived from the refractive index and structure profile. It relies on the fact that light passing through a transparent media undergoes a phase change as a function of its optical thickness (the refractive index times the physical thickness) [17]. Thus, light passing through the final coated profile of the mask has a different phase transmittance than light passing through the same thickness of air. The designed phase element of a diameter 'r' (in mm) and depth 'd', adds a phase on the input field expressed in equation (9):

$$\phi_i = \frac{2\pi md\left(n-1\right)}{\lambda} \quad (9)$$

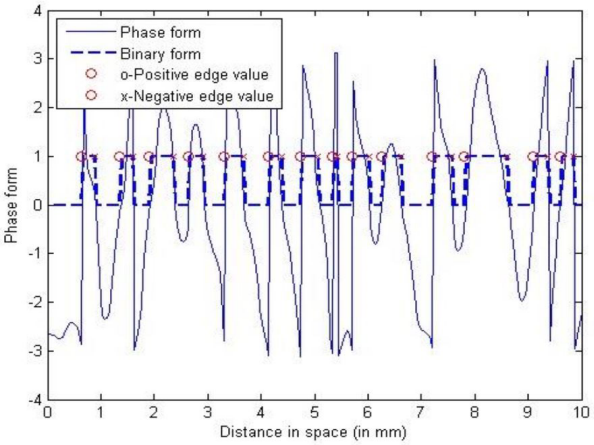

Fig.2: *Conversion of greyscale to binary pulses.*

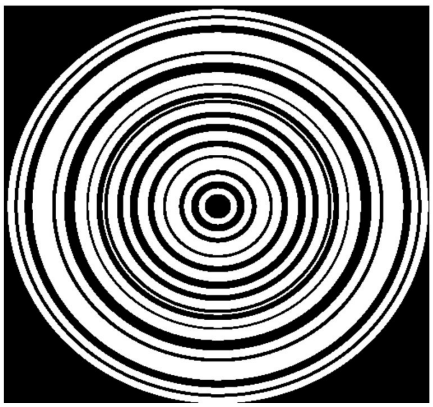

Fig.3: *Plot of the data of the binary form.*

where, 'n' is the refractive index of the material of the phase element and 'm' is an integer.

2.4 Conversion of Greyscale Masks to Binary Form

To achieve a STL format suitable for 3-D printing, the greyscale mask (from the simulations) needs to be converted to a binary form. This can be done by detecting positive and negative values in the greyscale image and assigning corresponding values of '0' and '1' respectively. In figure 2, the phase form of a greyscale mask is taken. The rising and falling edges are given value of 0 and 1. These edges are then plotted together in a radially symmetric fashion as depicted in figure (3). They are used and converted to generate the STL file.

2.5 Radial Phase Mask to STL Format for 3-D Printing

In order to realize the calculated phase mask, one needs to transfer phase information into difference in heights of different regions across the binary phase mask. A radial binary phase mask can be represented

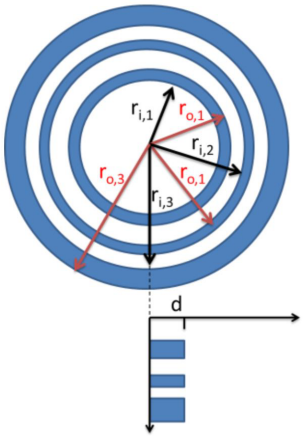

Fig.4: *Radial representation of a phase mask.*

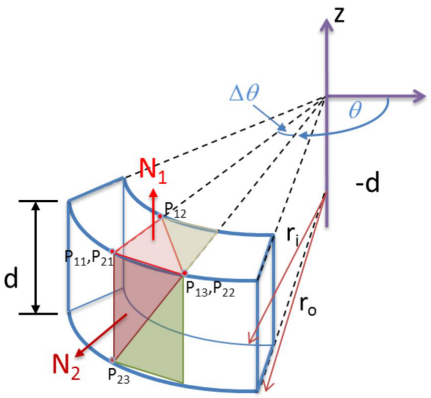

Fig.5: *Schematic for converting ring segment to triangular elements to compose the final STL format.*

by cylinders of different inner and outer radii as depicted in figure 4.

To convert to STL file format, each ring is then divided into segments of angular width of $\Delta\theta$ as shown in figure 5. Every segment is decomposed into eight triangular elements. Each element is defined by three points (P_{h1}, P_{h2} and P_{h3}) and a vector normal to the surface (N_h) where h is the element index.

For two highlighted elements in the graph (element 1 and element 2), one can define the end points of these elements as:

$$P_{11} = P_{21} = (r_o \cos(\theta + \Delta\theta), r_o \sin(\theta + \Delta\theta), 0) \tag{10}$$

$$P_{12} = (r_i \cos(\theta + \Delta\theta), r_i \sin(\theta + \Delta\theta), 0) \tag{11}$$

$$P_{13} = P_{22} = (r_o \cos(\theta), r_o \sin(\theta), 0) \tag{12}$$

$$P_{23} = (r_o \cos(\theta + \Delta\theta), r_o \sin(\theta + \Delta\theta), -d) \tag{13}$$

The two normal vectors are defined as:

$$\bar{N}_1 = (0, 0, 1) \tag{14}$$

$$\bar{N}_2 = \left(\sin\left(\theta + \frac{\Delta\theta}{2}\right), -\cos\left(\theta + \frac{\Delta\theta}{2}\right), 0\right) \quad (15)$$

Once the STL format of the phase mask is realized, the mask is printed using 3-D printer (Mini CR-7, Shenzhen Creality 3D Technology Co. Ltd, China) with transparent PLA filament.

2.6 Adhesion of The Transparent PLA with Glass

Following the printing of the simulated masks using transparent filament, another challenge to overcome is its adhesion to the glass substrate (glass slide in this case). The high printing temperature (210°C) set at the time of printing affects the attachment of the filament on the glass. As a result of which, the mask keeps shifting, overlapping and breaking. To solve this problem a transparent liquid glue can be applied to the glass slide. The excess of glue needs to be carefully drained. It requires to be evened out in order to remove air bubbles and reduce their interferences with the transparency of the phase mask.

2.7 Characterisation of the Samples

The characterisation of the sample is performed through the optical setup shown in figure 6. A red laser, with an operating wavelength of 650 nm, is used as the source with an attenuator comprised of two linear polarizers to prevent saturation on the CCD-array.

The next step is to fix the focusing lens which is formed by combining two lenses together. The phase element is then placed behind the two lens system. The focusing lens acts as a collimator and aligns the light as demonstrated in the characterisation setup.

Another crucial part is to align the imaging system in order to find the focusing point of the fabricated mask. Thereafter, the element is placed behind the focusing lenses and the camera located at the imaging plane. The camera is incrementally moved towards the lenses in fixed steps using an optical rail system and the images are recorded. The focusing point is measured without the designed optical element. A second measurement is performed after the element is placed. Figure 6 shows the operating distance from collimator to the camera is the focal length with the phase mask.

3. RESULTS AND DISCUSSION

The simulated greyscale phase mask is optimised with a phase factor of 0.9. This relatively gives a closer output profile to the flattop beam profile. The closeness is shown in figure 7. The similarity between the output beam of the simulation with the target is compared and observed to be greater than 95%.

This radial phase mask in figure 8.a converted to STL format is shown in figure 8.b. Figure 8.c is the 3-D printed realised phasemask using transparent PLA. The 3-D printer used for printing has a maximun resolution of 0.1 mm. which consequently affects the resolution of the printed phase mask.

There are several factors affecting the image in this setup like noise, camera alignment and resolution of the printed samples. Hence, the mean of the peak intensity is evaluated for both the x and y axis with respect to the distance over which the camera is moved. The source with the element can be observed to focus at a point 32D (where D = 2.5 cm) as shown in the figure 9.

After the optical element is aligned as described in section 2.7, the main aim is to focus the light efficiently in order to obtain a closer profile to the desired output (flattop). After empirical testing the image is observed to focus and give the profile as shown in figure 10. The y-axis represents the profile of the recorded image. This profile is compared with the simulation result of the phase mask of the output beam. It is evaluated through simulation in blue circle and the desired output in green square.

The results seen in the y-axis with the optical element in the experiment is quite close to the expected profile, which is higher than the 95% cross-correlation value shown in figure 11, which represent the simulation plot of the comparison between the output profile and target profile. Though high cross correlation value was obtained from the iteration process, obvious presence of ripples is observed. This pattern can be mainly attributed to the restricting constrain placed where radially symmetric binary phase profile was used.

4. CONCLUSION

In this paper, a low-cost, radially symmetric phase mask is designed through an iterative algorithm involving method of projection and cross-correlation for optimisation. The simulated masks are fabricated using 3D printing technique using transparent PLA filament. The optical properties of the fabricated mask are characterised and compared to simulations. This fabrication process eliminates the need of vacuum system and lithographic technique which reduces processing time and cost that is required for classical fabrication. It can be observed in the results that the element does change the focal point of the unmodulated source. When tested over varying distances from the lens, it gives a profile closer to the one obtained through the simulation.

This research can be further optimised by using higher resolution 3D printer. The adhesion of the element can be improved while printing. Moreover, more functionality such as vortex element can be added to the phase mask used for selective mode excitation using the proposed technique.

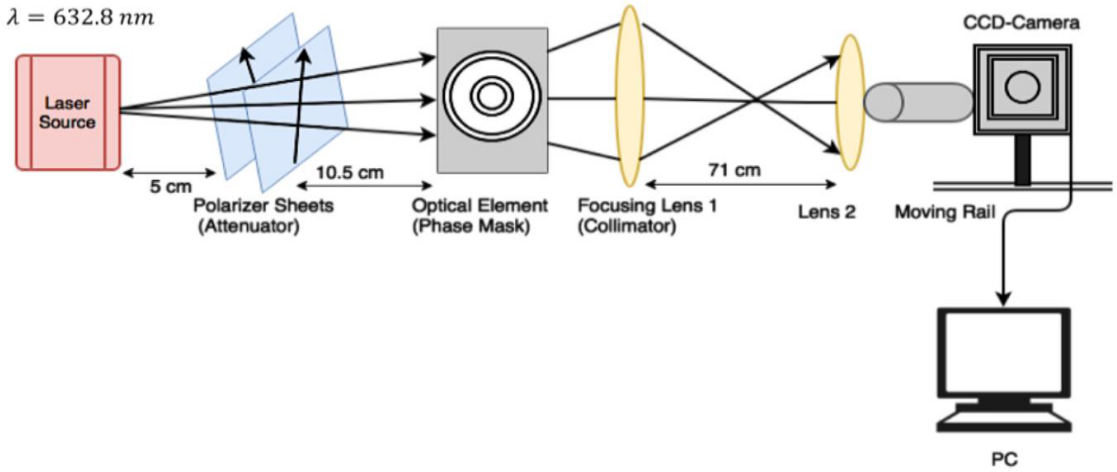

Fig.6: *Optical characterisation setup.*

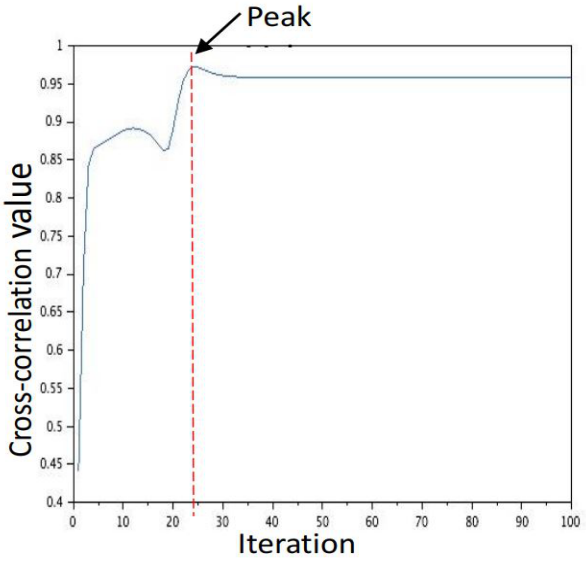

Fig.7: *Plot of cross-correlation versus number of iterations.*

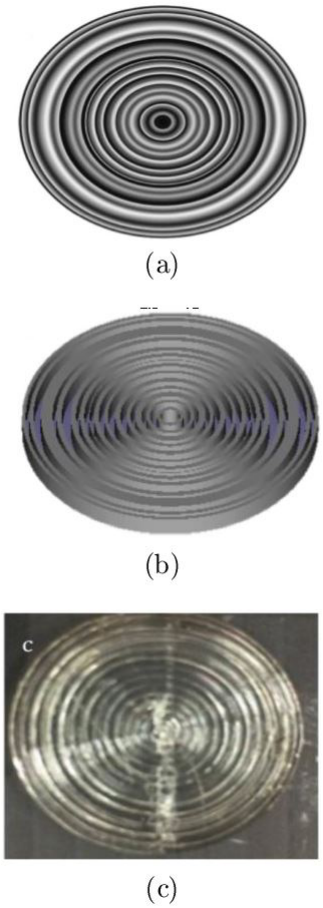

Fig.8: *a) Greyscale image of phase mask. b) STL image from greyscale. c) 3-D print of the phase mask.*

References

[1] G. Raciukaitis, E. Stankevicius, P. Gecys, M.Gedvilas, C. Bischoff, E. Jager, U. Umhofer, and F. Volklein, "Laser processing by using diffractive optical laser beam shaping technique," *J. Laser Micro/Nano eng.*, Vol. 6, No. 1, pp. 37-43, 2011.

[2] B. Baird, T. Gerke, K. Wieland, and N. Paudel, "P2 and P3 spatially shaped la- serscribing of CdTe and a-Si thin film solar cells using 532nm picosecond MOFPA," in Hamburg, Germany, *Proc. 26th European Photovoltaic Solar Energy Conference Exhibition*), Hamburg, Germany, pp. 2471-2474, Sep. 2011.

[3] C. Bischoff, E. Jäger, and U. Umhofer, "Beam Shaping Optics for Process Acceleration," *Laser*

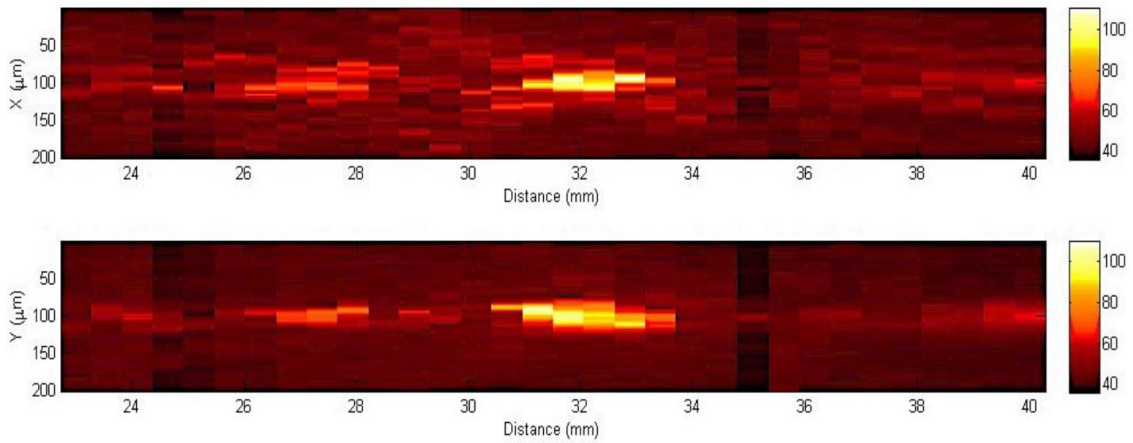

Fig.9: *Optical characterisation setup.*

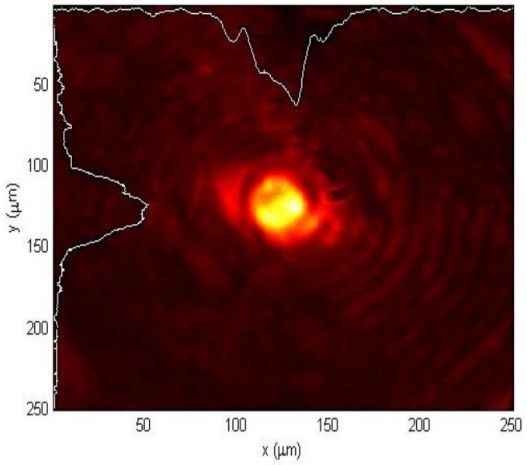

Fig.10: *Image of the light focused with the element(centered).*

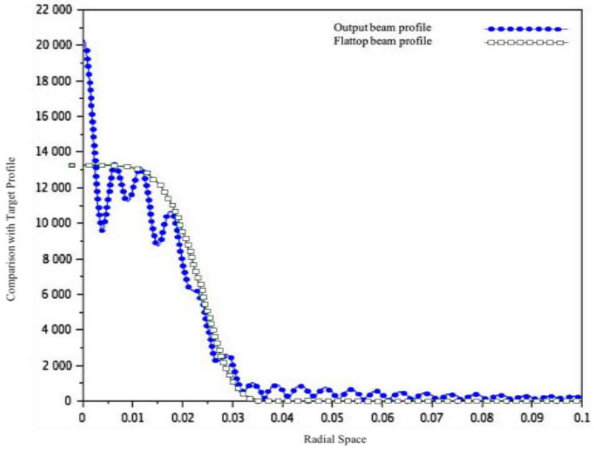

Fig.11: *Image of the light focused with the element(centered).*

Technik J., Vol. 12(3), pp. 53-57, 2015.

[4] J. Menapace, P. Davis, W. Steele, M.R. Hachkowski, A. Nelson, and K. Xin, "MRF applications: on the road to making large-aperture ultraviolet laser resistant continuous phase pates for high-power lasers," *Laser-Induced Damage Optical Materials, SPIE Proc.*, Vol. 6403, pp.6403-6413, 2007.

[5] C.C Aleksoff, K.K Ellis, and B.D. Neagle, "Holographic conversion of a Gaussian-beam to near-field uniform beam," *Optitcal Eng.*, Vol. 30, pp. 537-543 1991.

[6] J. A. Hoffnagle and C. M. Jefferson, "Design and performance of a refractive optical system that converts a Gaussian to a flattop beam," *Appl. Optics*, Vol. 39,(12), pp. 5488-5499, 2000.

[7] R. W. Gerchberg and W. O. Saxton, "A practical algorithm for the determination of phase from image and diffraction plane pictures," *Optik*, Vol. 35, pp.227-246, 1972.

[8] J. S. Liu and M. R. Taghizadeh, "Iterative algorithm for the design of diffractive phase elements for laser beam shaping," *Optics Letters*, Vol. 27(16), pp.1463-1465, 2002.

[9] Q. Li, H. Gao, Y. Dong, Z. Shen, and Q. Wang, "Investigation of diffractive optical element for shaping a Gaussian beam into a ring-shaped pattern," *Optics & Laser Technology*, Vol. 30, pp.511-514, 1998.

[10] J.W. Goodman, *Introduction to Optics,* Robert & Co, 2005.

[11] P. J. Smilie and T. J. Suleski, "Variable-diameter refractive beam shaping with freeform optical surfaces," *Optics Letters*, Vol. 36(21), pp.4170-4172, 2011.

[12] T. Gissibl, M. Schmid, and H. Giessen, "Spatial beam intensity shaping using phase masks on single-mode optical fibers fabricated by femtosecond direct laser writing," *Optica*, Vol. 3, No. 4, pp.448-451, 2016.

[13] V. A. Soifer, *Methods for Computer Design of*

Diffractive Optical Elements, Wiley, 2002.

[14] T. Bücкmann, N. Stenger, M. Kadic, J. Kaschke, A. Frölich, T. Kennerknecht, C. Eberl, M. Thiel, and M. Wegener, "Tailor 3D mechanical metamaterials made by dip-in direct-laser-writing optical lithography," *Advanced Materials*, Vol. 24(20), pp.2710-2714, 2012.

[15] M. Mizoshiri, H. Nishiyama, J. Nishii, and Y. Hirata, "Three-dimensional SiO2 surface structures fabricated using femtosecond laser lithography," *Appl. Physics A*, Vol. 98, pp.171-177, 2010.

[16]] R. M. Vázquez, S. M. Eaton, R. Ramponi, G. Cerullo, and R. Osellame, "Fabrication of binary Fresnel lenses in PMMA by femtosecond laser surface ablation," *Optics Express*, Vol. 19(12), pp.11597-11604, 2011.

[17] C. A. Mack, *Field Guide to Optical Lithography,* SPIE Press, Bellingham, WA, 2006.

Simran Agarwal Simran Agarwal received her Bachelor of Science in Engineering in Electronics from Asian institute of Technology, Thailand 2015. She received her Master in Electrical and Computer Engineering from Bangkok University, Thailand in 2018. Her research interests are diffractive optics, high power lasers, advanced precision fabrication and development of medical diagnostic tools.

Romuald Jolivot Dr. Romuald Jolivot received a B.Eng degree in Electrical and Electronic Engineering and Computer Vision in 2006 from Université de Bourgogne, France. In 2008, he received a joined Erasmus Mundus Master in Computer Vision and Robotics (ViBot) from Heriot-Watt University (UK), Universitat de Girona (Spain) and Université de Bourgogne (France). He obtained a Ph. D. degree in Instrumentation and Computer Vision in 2011. He is a researcher at the School of Engineering at Bangkok University, Thailand. His research interests include Computer vision; Image processing; Medical imaging; Multi/ hyperspectral imaging; Biomedical instrumentation.

Waleed S. Mohammed Dr. Mohammed graduated from the department of electronics and electrical communications, Faculty of Engineering, Cairo University, Giza, Egypt on 1996 with a major in control systems. In 1997, he joined the Lasers institute (NILES), Cairo University as a teaching assistant. He received M.Sc. degree from the department of computer engineering, Cairo University under the supervision of Prof. Adel El-Nadiand Prof. Ali Fahmy in 1999. In the same year he joined the College of optics and photonics/CREOL, University of Central Florida, Orlando, FL, USA as a research assistant. In 2001, he received M.Sc. degree in optics in 2001. He completed his Ph.D. work in 2004 and his thesis was titled "nano/micro optical elements for mode coupling applications. In 2004, he joined Prof. P. W. E. Smith's ultra-fast photonics laboratory (UPL), Electrical and Computer Engineering department, University of Toronto, as a postdoctoral fellow. In 2005, he joined Prof. Li Qian's group at the same University. In 2007 Dr. Mohammed joined the International school of engineering, Chulalongkorn University, Bangkok, Thailand as an instructor in the nano-engineering department. He taught optoelectronics, fundamental of optics, numerical modeling, nano-electronics and research methodology. As of September 2010, He joined the school of Engineering, Bangkok University as a research scholar.